Tropical Cyclone Outer Surface Winds Derived from Satellite Microwave Sounder Data

STANLEY Q. KIDDER,[1] WILLIAM M. GRAY AND THOMAS H. VONDER HAAR

Department of Atmospheric Science, Colorado State University, Ft. Collins, 80523

(Manuscript received 17 September 1979, in final form 26 November 1979)

ABSTRACT

Upper tropospheric temperature anomalies are detected in brightness temperature data from the Nimbus 6 Scanning Microwave Spectrometer (SCAMS). Brightness temperature anomalies are related to surface pressure anomalies through the radiative transfer and hydrostatic equation. Surface wind speeds at outer radii are then estimated using the gradient wind equation and a shearing parameter. The method is first tested using simulated satellite data constructed from temperature, pressure and height data recorded by aircraft reconnaissance of four hurricanes. Wind speeds in the 80–95 kPa region are estimated with 2–3 m s^{-1} accuracy. Next, 55.45 GHz SCAMS data over eight typhoons during 1975 are used to estimate the radii of 15.4 m s^{-1} (30 kt) and 27.5 m s^{-1} (50 kt) winds. Accuracies of about ±80 and ±70 km, respectively, are found. It is suggested that the technique be further tested using data from the Microwave Sounding Unit (MSU) on board the TIROS-N and NOAA 6 satellites.

1. Introduction

Over large areas of the oceans, the only feasible method for monitoring tropical cyclones is through the use of satelliteborne instrumentation. Since the launch of the first meteorological satellite in 1960, scientists have been collecting such data. Today the data are abundant and the challenge is to translate the raw data into accurate estimates of meteorological parameters.

One of the most important parameters of a tropical cyclone is surface wind speed. Among the uses of surface wind speed information are the following. Numerical models of storm motion need the wind speeds as input. Those responsible for routing ships need to chart courses which are outside the radius of 30 kt winds. Storm surge models are very sensitive to wind speed. Over the years a great deal of work has gone into the estimation of maximum sustained surface wind speed (intensity). The culmination of these efforts is the widely used Dvorak (1975) technique which is based on a correlation of intensity with cloud patterns. Unfortunately, the Dvorak technique does not estimate wind speeds at outer radii which are poorly related to intensity (see Gray and Frank, 1978, Tables 14 and 15). Recently, however, because of their importance to ship routing and storm surge prediction (Jelesnianski and Taylor, 1973), outer winds have become a topic of interest. Rodgers *et al.* (1979) have obtained good estimates of low-level wind speeds around tropical cyclones by tracking clouds in high-frequency (7.5 min) GOES (Geosynchronous Operational Environmental Satellite) images. Initial results from the Seasat-A Scatterometer System (SASS) and the Scanning Multichannel Microwave Radiometer (SMMR)[2], also on board Seasat, indicate that in the future, these instruments may be able to estimate surface wind speeds around tropical cyclones by observing the sea state (Jones *et al.*, 1979; Lipes *et al.*, 1979).

In a previous paper (Kidder *et al.*, 1978) we proposed a microwave technique for estimating surface wind speeds at outer radii which has several potential advantages over other techniques. First, it is suitable for use with the Microwave Sounding Unit (MSU) on board the current polar-orbiting operational satellites (TIROS-N and NOAA 6). Second, it requires only a small amount of computing and no special equipment, such as video displays. Third, it utilizes routinely available data; no special observations are needed. Fourth, the technique is unaffected by the extensive cloudiness which surrounds a tropical cyclone. And finally, it is an objective technique based soundly on the radiative transfer, hydrostatic and gradient wind equations. Note that in related work Grody *et al.* (1979) have used microwave data to estimate weighted mean tropospheric wind speeds around Typhoon June (1975).

In this paper we drive a more exact relationship between satellite-observed brightness temperatures and surface wind speeds than presented in Kidder

[1] Current affiliation: Laboratory for Atmospheric Research, University of Illinois, Urbana 61801.

[2] SMMR is also on board the Nimbus 7 satellite.

0027-0644/80/020144-09$06.25

et al. (1978). The theory is first tested using simulated satellite data constructed from aircraft reconnaissance of four hurricanes. The theory is next tested using data from the 55.45 GHz channel of the Nimbus 6 Scanning Microwave Spectrometer (SCAMS) to estimate the radii of 15.4 m s^{-1} (30 kt) and 25.7 m s^{-1} (50 kt) winds in eight West Pacific typhoons during 1975. We call this technique the Surface Wind Inference from Microwave data (SWIM) technique.

2. Theory

The high surface winds in a tropical cyclone are caused by surface pressure gradients which are in turn caused by warm temperature anomalies in the upper troposphere. The basis of the SWIM technique is that microwave radiometers can measure the upper level warming which may then be related to surface winds.

a. Tropical cyclone temperature structure

Shown in Fig. 1 are the mean temperature anomalies (difference from storm environment) for west Pacific typhoons and for Atlantic (West Indies) hurricanes as composited from rawinsonde data by Núñez and Gray (1977). The two main features of the curves are 1) the large positive anomalies peaking between 25 and 30 kPa and extending several hundred kilometers from the storm center, and 2) the remarkable similarity in the shape of the profiles at different radii. Specifically, the temperature anomaly is well approximated by

$$T'(r,z) = \alpha(r)\hat{T}(z), \qquad (1)$$

where $\hat{T}(z)$ is a standard known temperature anomaly profile (slightly different in the different oceans) and $\alpha(r)$ is a strength parameter, which will be different for different storms. That this relationship is not an artifact of the compositing procedure may be seen in plots of temperature anomalies in individual storms (e.g., in LaSeur and Hawkins, 1963; Hawkins and Rubsam, 1968; Hawkins and Imbembo, 1976).

It must be noted that the profiles shown in Fig. 1 have been modified slightly from those presented in Núñez and Gray (1977). First, because there were few statistically significant temperature anomalies at low levels, the profiles were extrapolated to zero at 100 kPa in the Pacific and at 70 kPa in the Atlantic. Second, small cold anomalies exist above the storms due to overshooting Cb cloud tops and/or radiative cooling. Because data are sparse at upper levels, this cooling was parameterized as follows. In the Atlantic, where storms are shallower than in the Pacific, the cooling was assumed to be zero at 16.25 kPa and 5 kPa and to be parabolic between with the amplitude determined by the 20 kPa anomaly such that the slope was continuous across 16.25 kPa. This parameterization fits the data rather well (see Kidder, 1979). In the Pacific, the cooling, shown schematically with the dotted line in Fig. 1a, was ignored because of statistical uncertainty in rawinsonde data at that altitude. It also made no difference in the calculations presented below.

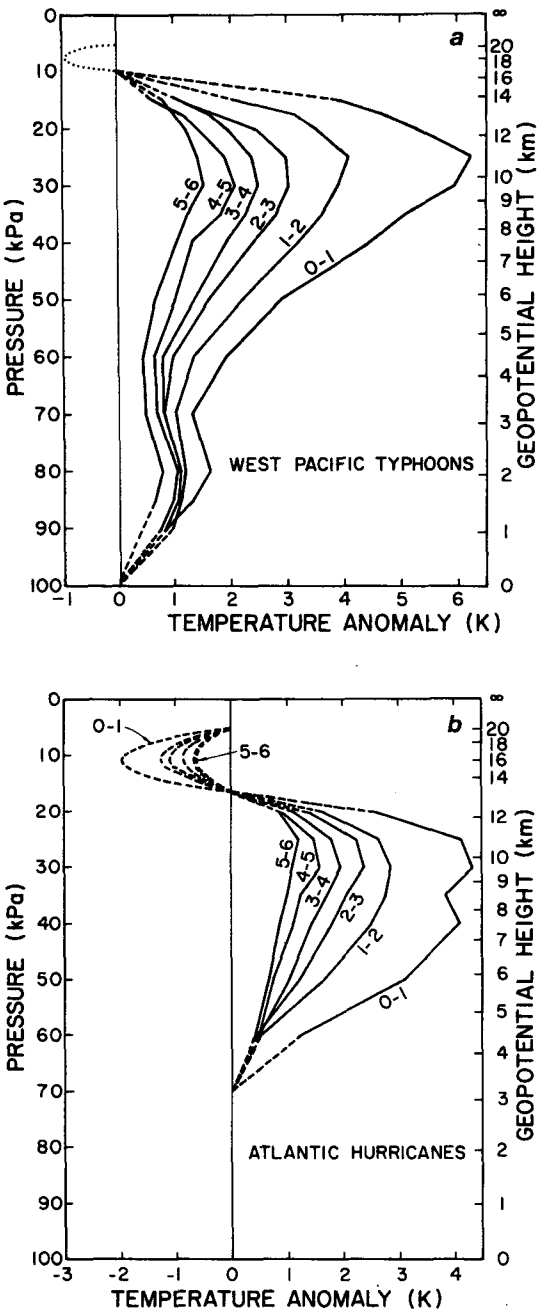

FIG. 1. Mean temperature anomalies in 1° radial bands for (a) West Pacific typhoons and (b) Atlantic (West Indies) hurricanes (after Núñez and Gray, 1977).

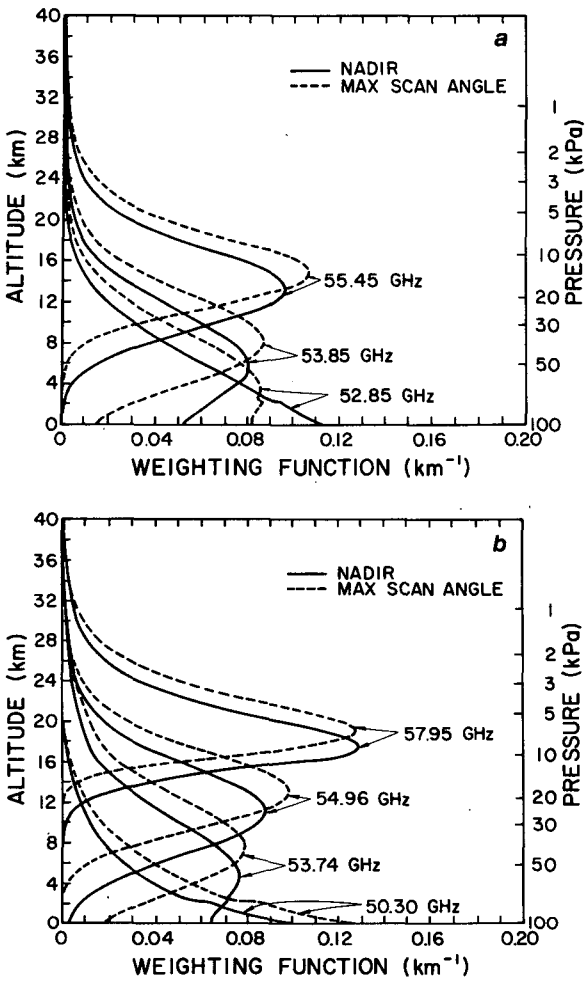

FIG. 2. Weighting functions for (a) the Nimbus 6 Scanning Microwave Spectrometer (SCAMS) and (b) the TIROS-N/NOAA Microwave Sounding Unit (MSU) in the 15° North Annual Atmosphere.

b. *Radiometer characteristics*

The SCAMS instrument is a five-channel radiometer sensing radiation nominally at 22.235, 31.65, 52.85, 53.85 and 55.45 GHz (Staelin *et al.*, 1975a). The lower two frequencies are used to estimate integrated liquid water and water vapor (Grody, 1976). The upper three channels, which are on the wing of an oxygen (O_2) absorption band, are used to sound the atmosphere. In the absence of scattering [due to particles of diameter ≥ 0.2 mm (i.e., precipitation)] the brightness temperature measured by channel $i (i = 3, 4, 5)$ of the radiometer is given by a form of the radiative transfer equation:

$$T_{B_i} = \epsilon_i T_s \tau_i + \int_0^\infty T(z) W_i(z) dz, \qquad (2)$$

where ϵ_i is the surface emittance, τ_i the transmittance from the surface to the satellite, T_s the surface temperature, $T(z)$ the atmospheric temperature at height z and $W_i(z)$ a weighting function (Staelin *et al.*, 1975a). $W_i(z)$ and ϵ_i are both weakly dependent on temperature but more strongly dependent on scan angle. Fig. 2 shows the weighting functions for the SCAMS and for the MSU on board the TIROS-N and NOAA 6 satellites. The 15° North Annual Atmosphere was used to construct these weighting functions, and it was assumed that the surface was the ocean where ϵ_i is ~ 0.5.

At frequencies which peak in the upper troposphere, warm brightness temperature anomalies should be observed over tropical cyclones. These warm anomalies were first observed in 55.45 GHz SCAMS data over Typhoon June of 1975 by Rosenkranz and Staelin (1976) and Rosenkranz *et al.* (1978) and over other storms by Kidder *et al.* (1978). All of the above authors concluded that the brightness temperature anomalies were not caused by clouds, which are far too transparent to cause anomalies of several kelvin (Staelin *et al.*, 1975b; Kidder, 1979) or by precipitation, which will be frozen (and thus much less able to interact with microwave radiation) at the levels sensed by the SCAMS 55.45 GHz channel. The brightness temperature anomalies are directly related to thermodynamic temperature anomalies in the storms as shown in Fig. 1. The object of this paper is to translate these satellite-observed brightness temperature anomalies into storm parameters of interest to the meteorologist.

c. *Surface pressure equation*

Warming in the upper troposphere is responsible for the surface pressure drop in tropical cyclones. Because satellite-measured brightness temperature (at certain frequencies) is a measure of this upper warming, brightness temperature ought to be related to surface pressure. It was shown in Kidder *et al.* (1978) that 55.45 GHz brightness temperature anomalies are statistically correlated with central pressure. A more exact relationship may be derived as follows. At a frequency for which the transmittance from the surface to the satellite is vanishingly small, the surface term in Eq. (2) may be neglected. Thus

$$T_B = \int_0^\infty T(z) W(z) dz. \qquad (3)$$

If the atmospheric temperature is divided into environmental temperature T_e plus temperature perturbation T', and if Eq. (1) is used to express T', we can write

$$T_B = \int_0^\infty T_e(z) W(z) dz + \int_0^\infty T'(r,z) W(z) dz \qquad (4)$$

or

$$T_B = T_{B_e} + \alpha(r) \int_0^\infty \hat{T}(z) W(z) dz, \qquad (5)$$

where T_{B_e} is the environmental brightness temperature. In the above, the small variation of the weighting function with temperature has been neglected.

The surface pressure outside of the radius of maximum wind can be obtained from the hydrostatic equation.[3] If the hydrostatic equation is integrated from the surface to a height such as the 5 kPa level which is undisturbed by the storm (Frank, 1977), we have

$$\ln p_s = \ln p_T + \frac{g}{R} \int_0^{H_T} \frac{dz}{T(z)} . \qquad (6)$$

Substituting for $T(z)$ as above and using the binomial expansion, keeping only terms linear in $\alpha(r)$, yields

$$\ln p_s = \ln p_e - \alpha(r) \frac{g}{R} \int_0^{H_T} \frac{\hat{T}(z)}{T_e^2(z)} dz, \qquad (7)$$

where p_e is the environmental surface pressure, and H_T the height of the 5 kPa surface. The unknown $\alpha(r)$ may now be eliminated between Eqs. (5) and (7) to yield

$$\Delta \ln p_s = -A \Delta T_B, \qquad (8)$$

where Δ indicates a departure from the environmental value and A is given by

$$A = \frac{\frac{g}{R} \int_0^{H_T} \frac{\hat{T}(z)}{T_e^2(z)} dz}{\int_0^\infty \hat{T}(z) W(z) dz} . \qquad (9)$$

Eq. (8) relates surface pressure anomalies to anomalies in a satellite-observed quantity (brightness temperature). Its usefulness depends on the characteristics of the coefficient A. Of chief concern is the uncertainty in the calculated value of A. An alternate method for calculating A which is slightly more accurate than Eq. (9) [because it takes into account the small variation of $W(z)$ with temperature] is to calculate the brightness temperature for a storm environment, then to perturb the environmental temperature with one of the profiles in Fig. 1 and calculate the surface pressure and brightness temperature anomalies. When this procedure was carried out using Pacific and Atlantic environmental soundings from the work of Núñez and Gray (1977) and atmospheric absorption coefficients calculated using the formulas of Liebe and Gimmestad (1978) and Liebe *et al.* (1977), the values of A listed in Table 1 resulted. There seems to be no systematic variation in A with radius, and the standard deviations of the samples are less than 10% of the mean values. Furthermore, A seems to be fairly insensitive to changes in the environment. Changing to the U.S. Standard Atmosphere changes A only ~12%. Similarly, switching an Atlantic temperature anomaly profile to a Pacific profile only changes A by ~11%. It thus appears that the coefficient A can be calculated from existing data, and it has a rather small uncertainty.

TABLE 1. Values of the coefficient A (K^{-1}) as a function of radius.

Radial band (deg latitude)	55.45 GHz	54.96 GHz
Atlantic		
0–1	1.13×10^{-2}	0.66×10^{-2}
1–2	1.10	0.66
2–3	1.07	0.64
3–4	1.03	0.62
4–5	1.01	0.62
5–6	0.94	0.54
6–7	0.85	0.51
Mean	1.02×10^{-2}	0.61×10^{-2}
Standard deviation	0.09×10^{-2}	0.06×10^{-2}
Pacific		
0–1	0.90×10^{-2}	0.82×10^{-2}
1–2	0.94	0.83
2–3	0.98	0.84
3–4	0.99	0.86
4–5	1.02	0.87
5–6	0.95	0.85
6–7	0.83	0.80
Mean	0.95×10^{-2}	0.84×10^{-2}
Standard deviation	0.06×10^{-2}	0.02×10^{-2}

Kidder *et al.* (1978) showed a high correlation (−0.86) between central surface pressure and the brightness temperature anomaly at the center of the storm. Although there are problems with this relationship due to the eye having a variable diameter, the high correlation is explained by Eq. (8).

d. Surface wind speed

If one has an estimate of the surface pressure gradient, one ought to be able to estimate the surface wind speed. Our simple approach to this problem is the following. Although surface pressure in tropical cyclones is nearly symmetric about the center (Frank, 1977), wind speeds are notoriously asymmetric. Most of that asymmetry at radii $\geq 1°$, however, can be explained by the motion of the storm (George and Gray, 1976). Therefore, we assumed that at gradient level (~85 kPa) the relative winds

[3] See Kidder (1979) for a demonstration that on space scales of 100 km the hydrostatic equation is valid in tropical storms.

(storm motion subtracted) were symmetric and to a close degree in gradient balance,[4] i.e.,

$$\frac{V_G^2}{r} + fV_G = RT_G \frac{\partial \ln p_s}{\partial r}, \tag{10}$$

where V_G is the relative wind speed at gradient level, r the radius, R the gas constant, T_G the temperature at gradient level, f the Coriolis parameter, and p_s the surface pressure. The surface pressure has been substituted for the pressure at gradient level because, by the hydrostatic equation, the radial gradient of the logarithms of the two pressures will be identical if the radial gradient of temperature between the two levels is small, which is the case (Fig. 1). Substituting from Eq. (8) yields

$$\frac{V_G^2}{r} + fV_G = -ART_G \frac{\partial T_B}{\partial r}. \tag{11}$$

Eq. (11) relates relative wind speed at gradient level to satellite-observed brightness temperature gradients.

If satellite data were noise-free, one could take any two brightness temperature observations near a tropical cyclone and estimate the gradient level wind speed between them from Eq. (11). Unfortunately, the SCAMS instrument has about ±0.5 K noise equivalent brightness temperature which would result in extremely noisy winds. It is therefore desirable to smooth the data before calculating the winds. One way to accomplish this smoothing is to assume a functional form for wind speed with radius. A suitably simple function proposed by Hughes (1952), Riehl (1954, 1963), and others is

$$V = Cr^{-x}. \tag{12}$$

The exponent x would be 1 for parcels conserving their angular momentum. Near the surface where friction is large, x is near 0.5 (Riehl, 1963; Gray and Shea, 1973). The effect of changing x will be discussed later. Inserting Eq. (12) in Eq. (11) and integrating with respect to r holding C, x, f, A and T_G constant, gives

$$T_B = (ART_G)^{-1}\left(C^2 \frac{r^{-2x}}{2x} - fC \frac{r^{1-x}}{1-x}\right) + T_c, \tag{13}$$

where T_c is an integration constant. Given a field of satellite-measured brightness temperature around a tropical cyclone, one can average the temperatures in radial bands about the storm center (an additional smoothing technique) and calculate the C which gives the best least squares fit to the data. This C is the real, positive root[5] of

$$\frac{1}{x^2}\left[\sum r^{-4x} - \frac{1}{N}(\sum r^{-2x})^2\right]C^3 - \frac{3f}{x(1-x)}\left[\sum r^{1-3x} - \frac{1}{N}(\sum r^{-2x})(\sum r^{1-x})\right]C^2$$
$$+ \left\{\frac{2f^2}{(1-x)^2}\left[\sum r^{2-2x} - \frac{1}{N}(\sum r^{1-x})^2\right] - \frac{2}{x}\left[\sum yr^{-2x} - \frac{1}{N}(\sum y)(\sum r^{-2x})\right]\right\}C$$
$$+ \frac{2f}{1-x}\left[\sum yr^{1-x} - \frac{1}{N}(\sum y)(\sum r^{1-x})\right] = 0, \tag{14}$$

where $y = ART_GT_B$.

One additional parameter is necessary. We used a simple shearing parameter to relate the surface wind speed to the wind speed at gradient level, i.e.,

$$V_s = \mu V_G. \tag{15}$$

Based on the work of Bates (1977) and Gray and Frank (1978), 0.7 was chosen as the value of μ. Because wind speeds above gradient level change slowly in comparison with those below gradient level (Frank, 1977; Bates, 1977), accurate knowledge of the height of the gradient level is not required.

The SWIM technique for estimating surface wind speeds from satellite-observed brightness temperatures can then be summarized as follows:

1) Average the brightness temperatures in radial bands about the storm center. [We used 56 km (½°) bands.]

2) Choose an appropriate value of x (see next section).

3) Calculate C with Eq. (14).

4) Calculate surface wind speeds using Eqs. (12) and (15).

5) Add the storm motion to the relative winds to obtain the asymmetric wind field.

The technique was tested using, first, simulated satellite data constructed from temperature, pressure and height data measured by hurricane reconnaissance aircraft, and second, using 55.45 GHz SCAMS data.

3. Results

a. Aircraft data

Although satellite data are prevalent over tropical cyclones, one invariably finds that the number of cases in which one has both satellite data and ground truth data is extremely small. Also ground

[4] This assumption is not true at the surface where friction is large. Surface wind speeds will be derived from gradient level wind speeds by a simple parameterization of frictional effects.

[5] It is observed that Eq. (14) has only one real, positive root. the other two are generally real and negative, although they are sometimes complex conjugates. Occasionally for weak storms, no positive real root is found.

TABLE 2. Summary of aircraft reconnaissance data from hurricanes used in this study.

Storm	Date	Flight levels (kPa)	Intensity change
Cleo	18 Aug 1958	80, 56, 24	Steady
Helene	26 Sep 1958	80, 56, 25	Deepening
Hilda	1 Oct 1964	90, 75, 65, 50, 18	Deepening
Hilda	2 Oct 1964	90, 70, 65, 20	Filling
Inez	28 Sep 1966	95, 75, 65, 50, 20	Deepening

resolution of microwave data is rather coarse—145 km at nadir for SCAMS, for example. For these reasons, we decided to first test the SWIM technique using simulated satellite data which had good ground truth data and high spatial resolution. Aircraft reconnaissance data collected for the National Hurricane Research Project (Gray and Shea, 1976) were utilized for this simulation. The data were screened for the following criteria: 1) There had to be at least three flight levels; 2) one of the flights had to be near the level of maximum warming (25–30 kPa); and 3) one of the flight levels had to be near the surface to measure low-level winds. Between 1957 and 1969 there were five days (four storms) on which such data were taken (Table 2).

The satellite data were simulated as follows. At each 4.6 km (2.5 n mi) radial grid point, smoothed

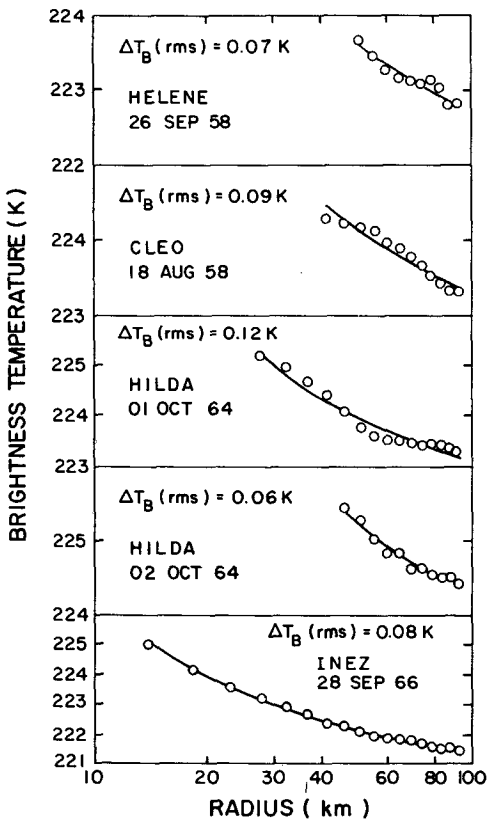

FIG. 3. Calculated 55.45 GHz brightness temperatures (circles) and best fit line for four hurricanes.

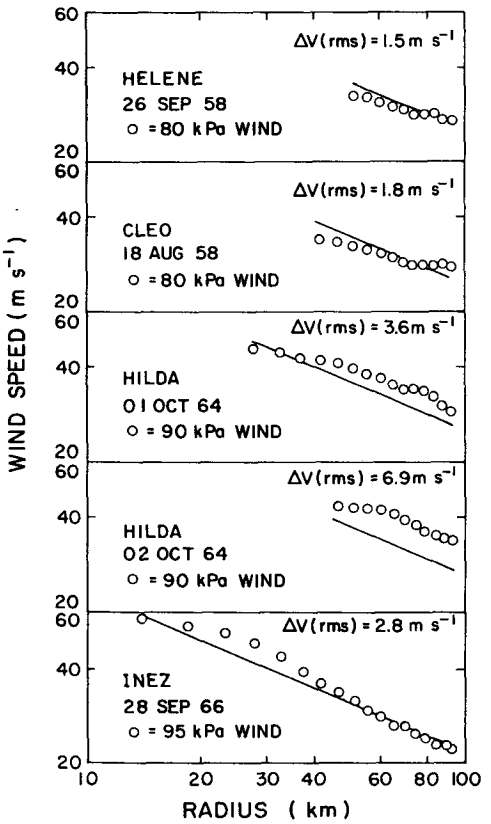

FIG. 4. Calculated gradient level (~85 kPa) wind speeds (line) and observed low-level wind speeds (circles) for four hurricanes (note that both scales are logarithmic).

vortex-averaged values of temperature, pressure and height (at the lowest flight level) from Gray and Shea (1976) and relative humidities from the mean hurricane environment (Kidder, 1979) were used to construct soundings. Between flight levels, the equivalent potential temperature was assumed to vary linearly with pressure (LaSeur and Hawkins, 1963), and above the uppermost flight level, the mean environmental sounding was used. Finally, 55.45 GHz brightness temperatures were calculated, from Eq. (2), for each grid point. The result was simulated, vortex-averaged, 55.45 GHz satellite data with a spatial resolution of 4.6 km (2.5 n mi).

Simulated data outside of the radii of maximum wind were inserted into Eq. (14) to calculate C for $x = 0.5$ and $A = 1.02 \times 10^{-2}$ K^{-1}. The offset T_c was also calculated, and the simulated brightness temperatures along with the best-fit line from Eq. (13) are shown in Fig. 3. It can be seen, particularly in the case of Inez, that Eq. (13) fits the data well. The wind speeds at gradient level (~85 kPa) were then calculated with Eq. (12), and they are compared with the observed, vortex-averaged wind speed at the lowest flight level (Fig. 4). With the exception of Hilda on 2 October 1964, the agreement between observed and calculated wind speeds is excellent with rms errors of 2–3 m s^{-1}.

TABLE 3. Typhoons used in this study (all 1975).

Name	Peak intensity ($m\ s^{-1}$)	Date/time (GMT) of peak intensity	Minimum sea level pressure (kPa)	Central location at time of peak intensity (°N)	(°E)
June	82	19 Nov/1200	87.5	13.2	141.0
Phyllis	62	14 Aug/1800	92.5	24.1	137.1
Rita	41	22 Aug/1200	—	32.9	134.4
Tess	49	4 Sep/1800	94.5	23.0	147.6
Winnie	33	10 Sep/0600	—	31.0	162.8
Alice	39	17 Sep/1200	97.3	15.4	132.1
Betty	49	22 Sep/0000	94.7	22.6	123.6
Cora	54	4 Oct/1800	94.3	30.3	133.2

The case of Hilda on 2 October 1964 is interesting because it is the only filling storm. It is possible that storm temperature structure is different enough in later stages that A should have a different value. It is also possible that the process of constructing soundings mentioned above failed to detect the true magnitude of the upper level temperature anomaly. This may have caused the calculated brightness temperature gradient, and thus the calculated winds, to be too low. More research is needed to adequately resolve this problem.

In summary, it appears that with 4–5 km resolution, low-noise satellite data, one could accurately deduce low-level tropical cyclone wind speeds. We next attempted to estimate wind speeds using Nimbus 6 SCAMS data.

b. Nimbus 6 data

In our previous study (Kidder *et al.*, 1978), we had collected 116 Nimbus 6 SCAMS images of hurricanes and typhoons during 1975. These images were screened to meet two criteria: 1) the scan angle to the storm center had to be less than or equal to 21.6°, and 2) an independent estimate of the radius of 15.4 m s^{-1} (30 kt) wind had to be available. Only 20 images met both criteria, and only one of these was in the Atlantic; the remainder were Pacific typhoons. To make the data set more uniform, Tropical Storm Gladys (the only Atlantic storm) was eliminated, leaving 19 images of eight typhoons (Table 3). This is a rather small data set but it is large enough to indicate the potential of the SWIM technique.

Before calculation of the wind speeds, the 55.45 GHz brightness temperatures were corrected for scan angle with an additive correction developed by Rosenkranz *et al.* (1978). The center of the storm was chosen as the maximum brightness temperature within 145 km (one scan spot) of the interpolated best track center (1975 Annual Typhoon Report). The brightness temperatures were then azimuthially averaged in 56 km (0.5° latitude) bands from 111 km (1°) to 778 km (7°). The brightness temperature in the very center of the storm was not used in the fitting process. Eq. (14) was used to calculate C for $x = 0.5$, $A = 0.95 \times 10^{-2}\ K^{-1}$ and $T_G = 17.2°C$. Finally, the radii of 15.4 m s^{-1} (30 kt) and 25.7 m s^{-1} (50 kt) winds were calculated using $\mu = 0.7$ to estimate surface wind speeds. These calculations are compared with observations in Fig. 5.

The observed radii were taken from logs kept at the Joint Typhoon Warning Center on Guam. Each 6 h the forecaster on duty estimates the radii of 30, 50 and 100 kt winds using all available data. There are two problems with these observations. First, they are not coincident in time with the satellite image. The observational values plotted in Fig. 5 have been averaged both around the storm and over the two 6 h estimates between which the satellite observation was made. Second, the observations are subjective estimates which introduces some variance and a bias. Because safety is the prime concern, the observations tend to be overestimates. The average value of this error is unknown.

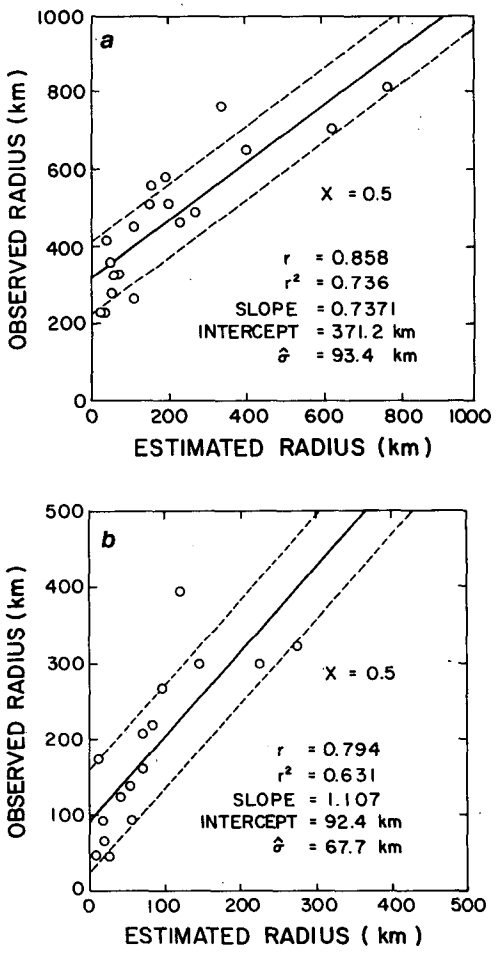

FIG. 5. Observed versus estimated average radius of (a) 15.4 m s^{-1} (30 kt) and (b) 25.7 m s^{-1} (50 kt) winds in eight typhoons during 1975 for $x = 0.5$.

The regression lines in Fig. 5 explain 63 and 74% of the variance for 25.7 m s^{-1} (50 kt) and 15.4 m s^{-1} (30 kt) winds, respectively. The standard errors of estimate are 68 and 93 km, respectively, which are reasonably good, and which may be influenced by the nature of the observed values. The intercepts are rather large, but some of this error is accounted for by the natural overestimation in the observed radii discussed above.

If the theory is correct, the slopes of the regression lines should be near 1. The fact that the slope for the radius of 15.4 m s^{-1} wind is somewhat less than 1 leads to speculation on the best value for the exponent x in the wind speed profile. Within 100 km of the storm center, 0.5 is a reasonable value for x, but Malkus and Riehl (1959) suggest that between 200 and 500 km x should be 0.6 to 0.7. Even though very few data points were available, an analysis was done to determine the effects of changing x.

Table 4 shows the square of the regression coefficient, the standard error of estimate, the slope and the intercept of the regression lines as functions of x. In general, increasing x slightly increases the fraction of explained variance, increases the slope, decreases the intercept and slightly decreases the standard error of estimate. For the radius of 25.7 m s^{-1} winds, an x in the range 0.4–0.5 produces the desired slope near 1.0. For the radius of 15.4 m s^{-1} winds, however, it appears that an x in the range 0.6 to 0.7 is a better choice. Fig. 6 shows the effect of changing x to 0.7. A better fit seems to be achieved for the radius of 15.4 m s^{-1} winds, but the opposite is true for the radius of 25.7 m s^{-1} winds. It appears, then, that for calculating the radius of 15.4 m s^{-1} (30 kt) winds by the SWIM technique one should use $x = 0.7$, but for the radius of 25.7 m s^{-1} (50 kt) winds one should use $x = 0.5$.

The 10% uncertainty in A causes approximately a 6–7% uncertainty in the wind speeds. The resultant uncertainty in the radius of a particular wind speed is the latter figure divided by x, i.e., a 13% uncertainty for $x = 0.5$ and a 10% uncertainty for $x = 0.7$. A better knowledge of the coefficient A would allow more accurate determinations of wind speed.

TABLE 4. Variation of regression statistics as a function of x.

x	r^2	Intercept (km)	$\hat{\sigma}$ (km)	Slope
	Radius of 15.4 m s^{-1} (30 kt) wind			
0.4	0.680	349	103	0.551
0.5	0.736	317	93	0.737
0.6	0.771	285	86	0.915
0.7	0.801	251	81	1.090
0.8	0.820	217	77	1.265
	Radius of 25.7 m s^{-1} (50 kt) wind			
0.4	0.579	111	72	1.058
0.5	0.631	92	68	1.107
0.6	0.663	74	65	1.165
0.7	0.685	55	63	1.231
0.8	0.701	36	61	1.305

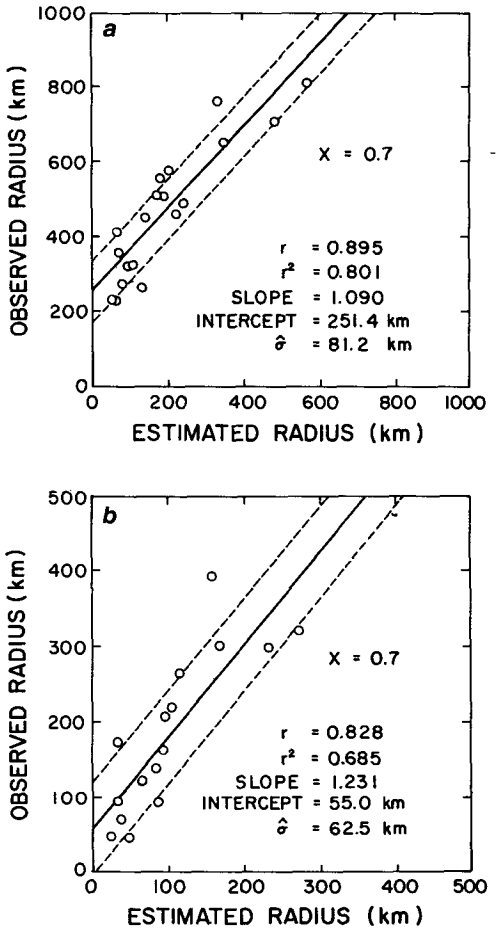

FIG. 6. As in Fig. 5 except for $x = 0.7$.

4. Conclusions

From Figs. 5 and 6, it appears that the SWIM technique is currently capable of estimating the radius of 15.4 m s^{-1} (30 kt) wind to within about ±80 km and the radius of 25.7 m s^{-1} (50 kt) wind to within about ±70 km. These results are promising, and indicate that further research is required.

The SWIM technique should be tried using TIROS-N and NOAA 6 data for several reasons. First, the MSU is a more sensitive instrument for estimating surface pressure gradients than was the SCAMS. The peak of the 54.96 GHz channel weighting function is closer to the peak of the temperature anomaly than the peak of the 55.45 GHz SCAMS weighting function (Fig. 2). Also, the 57.95 GHz channel could be used to measure the cooling above the storm. A two-parameter estimation of the sur-

face pressure anomaly of the form

$$\Delta \ln p_s = A\Delta T_{B_1} + B\Delta T_{B_2} \quad (16)$$

should be more accurate than a single-parameter estimation. Second, since the launch of NOAA 6 there are four images per day of tropical cyclones, about half of which pass closely enough to the storm center on the average to apply the SWIM technique. And finally, the TIROS-N/NOAA series are the current operational satellites from which microwave data are routinely processed in near real time. This technique is also suitable for use with the microwave sounder on board the new DMSP satellite, and further testing may be done with those data.

In summary, we think that the microwave technique described in this paper, which we have called the SWIM technique, has the potential to become a valuable tool at the disposal of the forecaster.

Acknowledgments. The authors would like to thank Sam Brand of the Naval Environmental Prediction Research Facility and David Sokol of the Joint Typhoon Warning Center for supplying data on the typhoons of 1975, and Hans J. Liebe of the U.S. Department of Commerce Office of Telecommunications for a computer program to calculate atmospheric transmittances. This research was sponsored by the National Aeronautics and Space Administration under Grant NSG-5258.

REFERENCES

Bates, J., 1977: Vertical shear of the horizontal wind speed in tropical cyclones. NOAA Tech. Memo. ERL WMPO-39, Miami, 19 pp.

Dvorak, V. F., 1975: Tropical cyclone intensity analysis and forecasting from satellite imagery. *Mon. Wea. Rev.*, **103,** 420–430.

Frank, W. M., 1977: The structure and energetics of the tropical cyclone I. Storm structure. *Mon. Wea. Rev.*, **105,** 1119–1135.

George, J. E., and W. M. Gray, 1976: Tropical cyclone motion and surrounding parameter relationships. *J. Appl. Meteor.*, **15,** 1252–1264.

Gray, W. M., and D. J. Shea, 1973: The hurricane's inner core region. II. Thermal stability and dynamic characteristics. *J. Atmos. Sci.*, **30,** 1565–1576.

——, and ——, 1976: Data summary of NOAA's hurricane inner-core radial leg flight penetrations 1957–1967, and 1969. Atmos. Sci. Pap. 257, Colorado State University, Ft. Collins, 219 pp.

——, and W. M. Frank, 1978: New results of tropical cyclone research from observational analysis. Naval Environmental Prediction Research Facility, Tech. Rep. TR-78-01, Monterey, 106 pp.

Grody, N. C., 1976: Remote sensing of atmospheric water content from satellites using microwave radiometry. *IEEE Trans. Antennas Propag.*, **AP-24,** 155–162.

——, C. M. Hayden, W. C. C. Shen, P. W. Rosenkranz and D. H. Staelin, 1979: Typhoon June winds estimated from scanning microwave spectrometer measurements at 55.45 GHz. *J. Geophys. Res.*, **84,** 3689–3695.

Hawkins, H. F., and D. T. Rubsam, 1968: Hurricane Hilda, 1964 II. Structure and budgets of the hurricane on October 1, 1964. *Mon. Wea. Rev.*, **96,** 617–636.

——, and S. M. Imbembo, 1976: The structure of a small intense hurricane—Inez, 1966. *Mon. Wea. Rev.*, **104,** 418–442.

Hughes, L. A., 1952: On the low level wind structure of tropical cyclones. *J. Meteor.*, **9,** 422–428.

Jelesnianski, C. P., and A. D. Taylor, 1973: A preliminary view of storm surges before and after storm modifications. NOAA Tech. Memo. ERL WMPO-3, 33 pp.

Jones, L. W., P. G. Black, D. M. Boggs, E. M. Bracalente, R. A. Brown, G. Dome, J. A. Ernst, I. M. Halberstam, J. E. Overland, S. Peterherych, W. J. Pierson, F. J. Wentz, P. M. Woiceshyn and M. G. Wurtele, 1979: Seasat scatterometer: Results of the Gulf of Alaska workshop. *Science*, **204,** 1413–1415.

Kidder, S. Q., 1979: Determination of tropical cyclone surface pressure and winds from satellite microwave data. Atmos. Sci. Pap. No. 307, Colorado State University, Ft. Collins, 87 pp.

——, W. M. Gray and T. H. Vonder Haar, 1978: Estimating tropical cyclone central pressure and outer winds from satellite microwave data. *Mon. Wea. Rev.*, **106,** 1458–1464.

LaSeur, N. E., and H. F. Hawkins, 1963: An analysis of Hurricane Cleo (1958) based on data from research reconnaissance aircraft. *Mon. Wea. Rev.*, **91,** 694–709.

Liebe, H. J., and G. G. Gimmestad, 1978: Calculation of clear air EHF refractivity. *Radio Sci.*, **13,** 245–251.

——, G. G. Gimmestad and J. D. Hopponen, 1977: Atmospheric oxygen microwave spectrum—experiment versus theory. *IEEE Trans. Antennas Propag.*, **AP-25,** 327–335.

Lipes, R. G., R. L. Bernstein, V. J. Cardone, K. B. Katsaros, E. J. Njoku, A. L. Riley, D. B. Ross, C. T. Swift and F. J. Wentz, 1979: Seasat Scanning Multichannel Microwave Radiometer: Results of the Gulf of Alaska workshop. *Science*, **204,** 1415–1417.

Malkus, J. S., and H. Riehl, 1959: On the dynamics and energy transformations in steady-state hurricanes. National Hurricane Research Project Rep. No. 31, Washington, DC, 31 pp.

Núñez, E., and W. M. Gray, 1977: A comparison between West Indies hurricanes and Pacific typhoons. *Postprints 11th Tech. Conf. Hurricanes and Tropical Meteorology*, Miami, Amer. Meteor. Soc., 528–534.

Rodgers, E. B., R. C. Gentry, W. Shenk and V. Oliver, 1979: The benefits of using short-interval satellite images to derive winds for tropical cyclones. *Mon. Wea. Rev.*, **107,** 575–584.

Riehl, H., 1954: *Tropical Meteorology*. McGraw-Hill, 392 pp.

——, 1963: Some relations between wind and thermal structure of steady-state hurricanes. *J. Atmos. Sci.*, **20,** 276–387.

Rosenkranz, P. W., and D. H. Staelin, 1976: Summary of operations: The scanning microwave spectrometer (SCAMS) experiment. *The Nimbus 6 Data Catalog*, Vol. 3, NASA/Goddard Space Flight Center, Greenbelt, 1–2 through 1–4.

——, —— and N. C. Grody, 1978: Typhoon June (1975) viewed by a scanning microwave spectrometer. *J. Geophys. Res.*, **83,** 1857–1868.

Staelin, D. H., A. H. Barrett, P. W. Rosenkranz, F. T. Barath, E. J. Johnson, J. W. Waters, A. Wouters and W. B. Lenoir, 1975a: The scanning microwave spectrometer (SCAMS) experiment. *The Nimbus 6 User's Guide*, NASA/Goddard Space Flight Center, Greenbelt, 59–86.

——, A. L. Cassel, K. F. Kunzi, R. L. Pettyjohn, R. K. L. Poon and P. W. Rosenkranz, 1975b: Microwave atmospheric temperature sounding: Effects of clouds on the Nimbus 5 satellite data. *J. Atmos. Sci.*, **32,** 1970–1976.

Staff, Joint Typhoon Warning Center, 1975: 1975 Annual Typhoon Report. Joint Typhoon Warning Center, COMNAVMARIANAS Box 12, FPO, San Francisco, 75 pp.